



# Durham E-Theses

---

## *The interactions of 88 MEV negative pi-mesons*

Allen, J. E.

### How to cite:

---

Allen, J. E. (1959) *The interactions of 88 MEV negative pi-mesons*, Durham theses, Durham University.  
Available at Durham E-Theses Online: <http://etheses.dur.ac.uk/10153/>

### Use policy

---

The full-text may be used and/or reproduced, and given to third parties in any format or medium, without prior permission or charge, for personal research or study, educational, or not-for-profit purposes provided that:

- a full bibliographic reference is made to the original source
- a [link](#) is made to the metadata record in Durham E-Theses
- the full-text is not changed in any way

The full-text must not be sold in any format or medium without the formal permission of the copyright holders.

Please consult the [full Durham E-Theses policy](#) for further details.

THE INTERACTIONS OF 88 MEV NEGATIVE PI-MESONS

By

J. E. ALLEN

Presented in candidature for the degree of  
Master of Science of the University of Durham.

Michaelmas, 1959.



## PREFACE

The material presented in this thesis concerns an examination of the interactions of  $\pi^-$ -mesons of 88 MeV kinetic energy with the nuclei of the various elements which constitute Ilford G5 emulsion. The experiment is the first of a series of four in which it is planned to examine the interaction characteristics of  $\pi^-$ -mesons in the energy range (100-800) MeV. Some of the results presented here have already been published. (Allen et al, 1959)

In the following pages, an outline of the main features of  $\pi$ -meson interactions with free nucleons is given first as being pertinent to the discussion which follows of meson interactions with complex nuclei. A consideration is then made of previous work and the need for further clarification. The optical model of the nucleus is dealt with in some detail as well as some relevant aspects of emulsion technique. There follow details of the experimental procedure, and the presentation and discussion of the results.

CONTENTS

	Page
List of Figures	iv
List of Tables	v
 Chapter 1. <u>THE INTERACTING PROPERTIES OF <math>\pi</math> - MESONS</u>	
1.1 Introduction.	1
1.2 The Scattering of $\pi$ -mesons by Nucleons	1
1.3 $\pi$ -meson Interactions with Complex Nuclei	3
1.31 General Considerations.	3
1.32 Inelastic Scattering	5
1.33 Absorption.	9
1.4 The Present Experiment.	12
 Chapter 2. <u>THE OPTICAL MODEL OF THE NUCLEUS</u>	
2.1 Introduction.	14
2.2 The Theory of the Model.	15
2.3 Application to Nuclear Emulsion	19
 Chapter 3. <u>SOME ASPECTS OF NUCLEAR EMULSION TECHNIQUE</u>	
3.1 Processing of Emulsions.	21
3.2 Measurements in Emulsion	25
 Chapter 4. <u><math>\pi</math>-MESON INTERACTIONS AT 88MEV</u>	
4.1 Experimental Details	29

	Page
Chapter 4 (contd).	
4.2 Contamination	31
4.3 Experimental Results	32
4.31 The Interaction Lengths	32
4.32 Comparison with the Optical Model.	33
4.33 The Inelastic Interactions	37
Chapter 5. <u>CONCLUSION</u>	47
<u>ACKNOWLEDGEMENTS</u>	48
<u>REFERENCES</u>	49

LIST OF FIGURES

	Facing page
1. The variation of the total cross-section for the interaction of positive and negative $\pi$ -mesons with hydrogen over the energy range (0 - 4500)MeV.	2
2. The ratio to the total inelastic cross-section of the cross-sections for absorption, charge exchange and inelastic scattering for $\pi$ -meson interactions with complex nuclei in the energy range (0 - 1000) MeV.	12
3. The variation of the interaction length with absorption co-efficient.	33
4. The observed distribution of horizontally projected angles of elastic scattering per $10^0$ interval together with curves computed from the optical model for various assumed values of the change in wave number.	33
5. The energy distribution of the inelastically scattered mesons.	41
6. The angular distribution of the inelastically scattered mesons.	42

LIST OF TABLES.

	Page
1. Values of $V_r$ and $V_i$ from experiments at energies close to 88 MeV.	36
2. Distribution of star sizes according to $n_h$ and $n_s$ .	37
3. Distribution of star sizes according to $n_h$ and $n_\pi$ .	38
4. Values of the mean number of prongs, $\bar{n}$ , for stars with and without meson secondaries at 120 MeV. (Ferrari et al, 1956) and 88 MeV. (present work).	38
5. Distribution according to $n_h$ of stars with one or more prongs in which meson absorption has occurred at rest, and absorption or charge exchange at 88 MeV.	40
6. Values of the mean energy loss, $(\overline{\Delta E})$ , of the secondary mesons and the mean number of prongs, $\bar{n}$ , of the star of origin, with a division into two equal groups according to the greater or lesser energy loss of the meson.	42
7. Values of the forward to backward ratio, F/B, and the mean number of prongs for black, grey and all heavy prongs of the 101 stars.	44

## CHAPTER 1

### THE INTERACTING PROPERTIES OF $\pi$ -MESONS

#### 1.1 Introduction.

The study of the interactions of  $\pi$ -mesons with atomic nuclei has become one of the accepted means of elucidation of details of nuclear composition. In its peculiar role as the quantum of the nuclear field, the  $\pi$ -meson has retained its fundamental importance despite the growing body of information which accumulates around the other 'fundamental' particles. Meson field theory depends for its verification on knowledge gained in studying the strong interactions of  $\pi$ -mesons and nucleons with both free nucleons and atomic nuclei. While it remains as yet not possible to give an exact formulation for the meson field, the most important theoretical work has been concerned with the meson-nucleon interaction as this would appear to afford the most simple and rewarding approach to the problem.

Since it is with  $\pi$ -meson interactions that this thesis is concerned, a broad outline of their essential features as known at present will be given.

#### 1.2. The scattering of $\pi$ -mesons by nucleons.

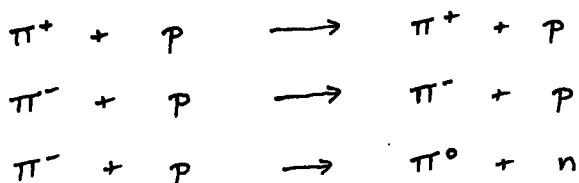
The availability of  $\pi$ -mesons of both signs and of a wide range of energies has made possible large numbers





of experiments on the scattering of  $\pi$ -mesons by hydrogen, which involves the meson-nucleon interaction in its simplest form. The variation with meson energy in the range (0-4500) Mev of the total cross-sections  $\sigma_{\pi p}$  and  $\sigma_{\pi \bar{p}}$  are shown in Fig 1. The data for this figure are from Yuan (1956), with additions from Burrowes et al (1959). On the basis of charge independence (conservation of isotopic spin) a satisfactory qualitative, and in part quantitative, account of the observed magnitudes of the cross-sections has been given. (see Bethe and de Hoffman, (1956); Lindenbaum (1957).).

The most probable interactions below 800 MeV and neglecting radiative capture, are:-



of which the first two represent elastic scattering and the third charge exchange scattering. Isotopic spin<sup>analysis</sup> shows that the first entails a pure  $T = \frac{1}{2}$  spin state while the second and third are complementary mixtures of the  $\frac{1}{2}$  and  $\frac{3}{2}$  states. From the maxima in the curves at about 200 MeV the existence is inferred of an excited nucleonic state; the apparent resonance is in a state of isotopic spin  $\frac{1}{2}$  and angular momentum  $\frac{1}{2}$ . The magnitudes of these maxima in the cross-sections are accounted for by the  $\frac{1}{2}$  resonance,

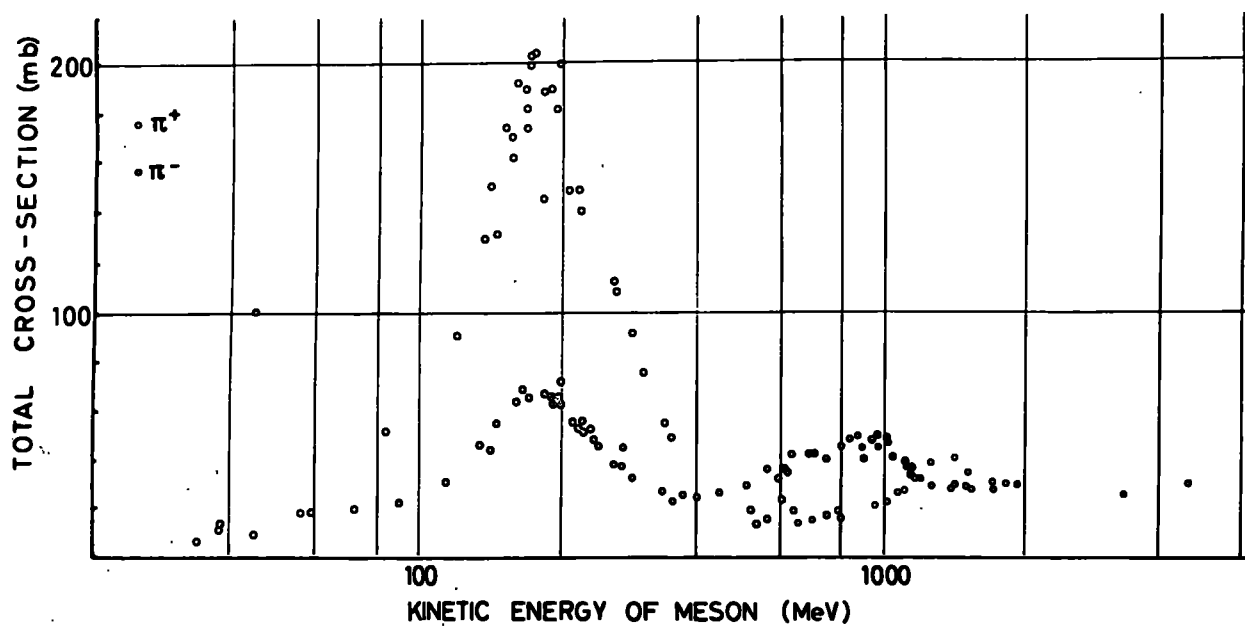


Fig.1. The variation of the total cross-sections for interaction of  $\pi^\pm$ -mesons in hydrogen.

the ratio of the  $\pi^+$  to the  $\pi^-$  cross-sections, 3 to 1, being equal to the proportion of the  $T=\frac{1}{2}$  state which contributes to the  $\pi^-$  cross-section. (At this energy the contribution from  $T=\frac{1}{2}$  is negligible).

Other less striking maxima are apparent in the curves at higher energies; that at about 900 MeV for the  $\pi^-p$  cross-section has been shown to be a double peak (Burrowes et al, 1959), and both are interpreted as resonances in a  $T=\frac{1}{2}$  state. The magnitude of the resonant cross-sections are found by subtraction of the  $T=\frac{1}{2}$  contribution obtained from the  $\pi^+$  cross-section. The peak at about 1300 MeV in the  $\pi^+$  curve is similarly thought to be due to a second  $T=\frac{1}{2}$  resonance. Exact interpretations at these high energies are complicated by the increasing number of possible angular momentum states, and other explanations, for example, in terms of a meson-meson resonance in a  $T=0$  state, have been put forward.

### 1.3 $\pi$ -Meson Interactions with Complex Nuclei

#### 1.31. General Considerations

It is convenient to divide the interactions of mesons with nuclei into two broad classes; elastic, in which there is very little energy transfer and the nucleus is unaffected by the collision, and inelastic, where greater amounts of energy transfer are involved and the nucleus becomes excited. The first type result from a deflection

result of collisions between the incident particle and the nucleon may be the production of one or more  $\pi$ -mesons. Evidence for the correctness of this cascade mechanism has come from experimental work on the interactions of mesons with nuclei.

### 1.32 Inelastic Scattering

$\pi$ -meson interactions with increasingly complex nuclei would be expected to show successively larger departures from the simple form of the meson-nucleon cross-sections already described. In the simplest case it is found that the total cross-section for  $\pi$ -mesons on deuterium,  $\sigma_{\pi^0D}$ , can be represented by the sum of  $\sigma_{\pi^0p}$  and  $\sigma_{\pi^0n}$ , (the latter is equal to  $\sigma_{\pi^0p}$  by charge symmetry) with the inclusion of a small correction term to account for interference effects (Ashkin et al, 1954; Cool et al, 1956). Support for the principle of charge symmetry is given by the apparent equality of  $\sigma_{\pi^0D}$  with  $\sigma_{\pi^0p}$ . For elements between beryllium and oxygen the resemblance persists with the curve corresponding to fig. 1. becoming flatter and broader in the resonance region (Ignatenko, 1956). This is in part due to the Fermi motion of the nucleons, which leads to a Doppler broadening effect. The incident meson may also suffer a preliminary scattering on one or more individual nucleons, losing energy in the process, and

it will then interact with the cross-section appropriate to its new energy; the effect of this is to smooth out the energy variations of the total cross-section.

Further evidence for the interaction of the meson with the individual nucleons of the nucleus is obtained from the study of the energy and angular distributions of  $\pi$ -mesons scattered inelastically on various nuclei. Ignatenko, reporting Russian work in the energy region (140-400)MeV, and other workers in the range, (Morrish, 1953; Miller, 1957; Belovitski, 1959; Wang et al, 1959) have observed that, in lighter nuclei, e.g., carbon, the angular distribution differs little from that expected for  $\pi$ -meson scattering on free nucleons. For heavy nuclei, however, e.g., lead, or silver, and bromine in nuclear emulsion, the distribution for small angles is quite different, though in the backward direction there is again considerable resemblance. First collisions in these heavy nuclei may be expected to occur just within the nuclear surface; thus a backward scattered meson will in general have suffered a single collision, whereas multiple collisions are probable for a forward scattered meson. It is further observed that for increasingly heavy nuclei the number scattered in the forward direction diminishes steadily.

The energy loss sustained by a meson in traversing a heavy nucleus is of the order of the maximum possible

energy transfer for a collision with a single nucleon , which is interpreted by Ignatanko as evidence for multiple collisions. Mesons emerging in the backward direction have in general lost less energy than others, which fact supports the ~~same~~ conclusion. Belovitskii has suggested the interaction of the meson with nucleon complexes in the nucleus as a means of accounting for the smaller energy loss in this case.

Observations in nuclear emulsion at higher energies are generally consistent with the idea of multiple collisions. The large energy loss sustained by escaping mesons remains a striking feature of the interaction. At 500 MeV, (Blau and Caulton, 1954), the energy spectra for secondary mesons emitted in the various angular intervals are not significantly different, and this obliteration of the features of scattering on single nucleons is most likely due to repeated multiple collisions. Lock and Yekutieli (1952), working with stars produced by mesons of cosmic origin in the energy range (50-1100) MeV, also observed the large energy loss suffered by the escaping particle. Comparing the characteristics of meson and proton induced stars they concluded that the cascade in the nucleus is initiated by successive collisions of the incident meson rather than by the secondary nucleons. It is suggested (Blau and Oliver, 1956), however, that the strong angular correlations observed are not consistent

with the idea of repeated multiple scattering and that an alternative mechanism for large energy loss in a single collision could be provided by the production and re-absorption of secondary mesons.

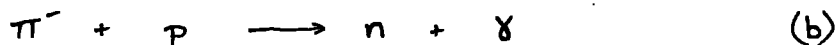
At energies approaching 1 GeV production of mesons becomes an important feature and the qualitative picture of the inelastic interaction is made more complicated. However, Metropolis et al (1958) have found it possible to make extensive Monte-Carlo calculations based on the cascade model for a range of incident meson energies. They employed experimental values of the various meson-nucleon cross-sections and included the effects of meson production and re-absorption. At 500 MeV, agreement with experiment is excellent with regard to the frequency of different types of event, but a smaller energy loss than that observed is predicted for escaping mesons together with an angular distribution more biased in the forward direction. At 162 MeV, a comparison with the results of Nikolskii et al (1957) reveals a reasonable agreement with the energy spectrum of the secondary mesons after allowance is made for an attractive meson-nucleus potential of the same magnitude as observed experimentally. The predicted angular distribution is again more seriously in error, having too great a bias in the backward direction.

In contrast the Bologna group (Ferretti et al, 1956) have reported fairly good agreement between a Monte-Carlo calculation and experimental results of the energy losses and angular distributions of inelastically scattered mesons at several energies between 62 and 120 MeV. At the low energy value single nucleon collisions were found sufficient for explanation of the results; at 120 MeV a substantial contribution from double scattering was invoked.

Thus while the cascade model appears to some extent an over-simplification, it has achieved a moderate success, and especially at low energies, the true mechanism may be expected to differ from it only in detail.

### 1.33 Absorption

For the absorption of zero energy  $\pi^-$ -mesons in hydrogen, the basic reactions are :-



and these occur with about equal probability. In deuterium and heavier nuclei, a more important process is



Here the binding energy of the nuclei does not permit reaction (a). Reaction (b) becomes rare, since most of the energy is taken by the  $\gamma$ -ray and the exclusion principle forbids the production of a low energy neutron. The dominant



reaction is thus absorption by a proton in nucleon groups of two or more to provide for momentum conservation. For light emulsion nuclei there is evidence (Manon et al, 1950; Clark and Ruddlesden, 1951; Demeur et al, 1956) that the meson interacts with the nucleons in  $\alpha$ -particle groupings (together with a deuteron in the case of nitrogen), and one or more of these may be disrupted as a result. For the heavier nuclei, the excitation energy given to the nucleus is of a lower order compared with the binding energy and, as described by the evaporation theory (Le Couteur, 1950), this is shared among the large number of individual nucleons independently of the meson interaction.

Absorption of non-zero energy mesons into the nucleus has been logically considered by Brueckner et al (1951) to be the inverse of the meson production processes; that is, by a nucleon pair, the pair to contain at least one proton for  $\pi^-$ -meson absorption, and one neutron for  $\pi^+$ -meson absorption. The two absorbing nucleons will carry away the rest energy of the meson of about 140 MeV, and the nucleus will be further excited by any scattering that occurs as they leave it.

In order to test this hypothesis of the absorption mechanism, assumed in his calculations, Metropolis compared the predictions for  $\sigma$ -star characteristics, i.e., absorption

of zero energy mesons, with the experimental results of Azimov et al (1957). The agreement obtained was limited, suggesting, as outlined above, that in this case other absorption mechanisms are possible - on single low energy nucleons or on more complex groups such as  $\alpha$ -particles.

At 750 MeV, Blau and Oliver observed a strong angular correlation of heavily ionizing tracks at right angles to the direction of the incident meson, which was interpreted as evidence for the interaction and absorption of mesons with nucleon complexes inside the nucleus. This conclusion is not necessarily in conflict with observations at lower energies.

Tomasini (1956), in a study of the absorption of bound  $\pi^-$ -mesons, found that limited agreement between the experimental results and a simplified Monte-Carlo calculation could be obtained by assuming that the absorption took place preferentially on a proton-neutron pair rather than on a proton-proton pair.

It still remains for calculations to be made assuming the simultaneous existence of other absorption mechanisms but it would appear that absorption on nucleon pairs is certainly the most important process for non-zero energy mesons.

#### 1.4. The Present Experiment

The cross-sections below 1 GeV as they are at present known for the inelastic interactions of  $\pi$ -mesons with complex nuclei are shown in Fig 2. They have been separated into those for absorption, for charge exchange scattering and for inelastic scattering, and plotted as the ratio of the cross-section  $\sigma$  to the total inelastic cross-section  $\sigma_i$ . The points on the graphs have been taken from experiments performed at a single energy in a variety of media and with machine produced beams; where not explicitly given in the paper, the values have been estimated from the presented results.

It can be seen that, within the energy range shown, all three cross-sections vary greatly; at low energies absorption is complete, whereas at 700 MeV it has become negligible and the probabilities of charge exchange and inelastic scattering are about equal. However, results from similar experiments exhibit wide variations, and at some energies only one particular aspect of the interaction has been examined. Attempts on a small scale to determine the variation in a single medium of the interaction parameters were made by Lock and Yekutieli (1952) and Major and Parkash (private communication), who each examined about 80 interactions produced by cosmic ray mesons. Their results have also been included in Fig. 2.

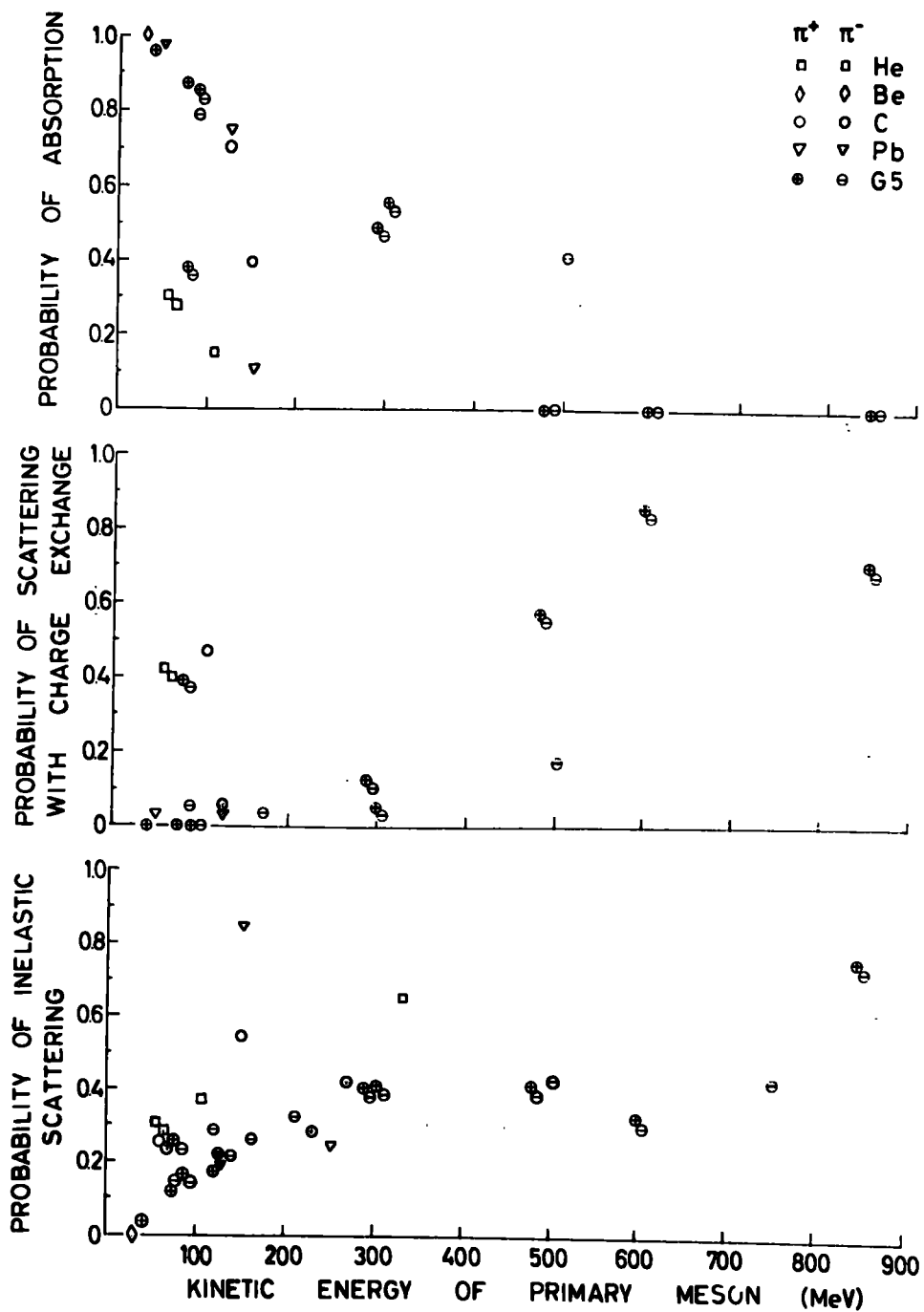


Fig.2a,b,c. The relative probabilities for the interactions of  $\pi^\pm$ -mesons with complex nuclei.

It was thought, therefore, that a useful purpose would be served if a more extensive investigation were carried out of the features of meson interactions in one material over a range of energies. The upper limit was fixed at 800 MeV since, as has already been mentioned, the cross-section for meson production becomes significant at higher energies and any analysis is thus made more complicated. As a reliable method of determination of the inelastic cross-sections it was decided to employ only scanning along the meson tracks. This method would necessarily produce a large number of elastic scattering events which could be compared with the predictions of the optical model. Exposures of four blocks of G5 emulsion at energies of approximately 100, 300, 500 and 700 MeV were proposed, the choice of  $\pi^-$ -mesons rather than  $\pi^+$  being made solely on account of availability of suitable beams. This, the first exposure of the series, was performed at 88 MeV.

## CHAPTER 2

### THE OPTICAL MODEL OF THE NUCLEUS

#### 2.1 Introduction

The interpretation of data on the scattering of mesons and nucleons by nuclei has been carried out with considerable success on the basis of the optical model of the nucleus. In this, an extension of a simple potential well model, the nucleus is considered to appear to the incident particle as a well of complex potential or, alternatively, as an homogeneous medium of complex refractive index. The incident particle wave is refracted, attenuated or diffracted by the complex potential, the real component being associated with elastic diffraction scattering and the imaginary component with inelastic processes including absorption. The results are obtained in terms of three parameters:  $K$ , the absorption co-efficient in nuclear matter,  $k_1$ , the change in wave number on entering the nucleus, and  $R$ , the radius of the potential well. The form of the potential employed is a uniform square well; at higher meson energies better agreement has been obtained with a tapered well (Williams, 1956) but this refinement will not be attempted here.

## 2.2. The Theory of the Model

If the reduced wave number of the incident meson wave is  $k$ , this is increased by the real component of potential in the nucleus,  $V_r$ , to  $k'$ , where in the non-relativistic case (Fernbach et al, 1949)

$$k' = k \left( 1 + V_r/E \right)^{\frac{1}{2}} \quad (1)$$

Relativistically, this expression becomes (Fowler and Perkins, private communication)

$$k' = k \left[ 1 + 2V_r/p\beta c + (V_r/pc)^2 \right]^{\frac{1}{2}} \quad (2)$$

where  $E$  is the kinetic energy of the meson;  $p$ , the momentum and  $\beta c$  the velocity. When  $V_r$  is small compared with  $E$  and  $p$ , these equations may be written respectively as

$$k_1 = k V_r / 2E \quad (3)$$

$$k_1 = k V_r / p\beta c \quad (4)$$

where  $k_1$  is  $(k' - k)$  the change in wave number.

Interference occurs between the refracted and the original wave fronts and a diffraction pattern is produced. An attractive or repulsive real potential will lead to corresponding positive or negative values of  $k_1$ . The resultant diffraction pattern is the same for phase changes of either sign; hence neither the sign of  $k_1$  nor that of the potential can be determined from the diffraction effect.

The relationship between the imaginary component of potential  $V_i$  and the attenuation length of the meson

wave  $\lambda_n$  is given by  $\lambda_n = \hbar \beta c / 2 V_i$  (5)

$\lambda_n$  is also the mean free path for interaction within the nucleus, and its reciprocal is the absorption co-efficient K.

K may be expressed in terms of the known cross-sections on free nucleons by assuming that, for the purposes of the optical theory, either inelastic scattering or absorption is the dominant interaction process within the nucleus. At 88 MeV absorption is expected to be the more important of the two, but it will be seen that in either case a similar result is obtained.

Considering first the scattering on individual nucleons, the absorption co-efficient<sup>is</sup> given by

$$K = 3A/4\pi R^3 \cdot [Z\sigma_{\pi p} + (A-Z)\sigma_{\pi n}] / A \quad (6)$$

in terms of the cross-sections  $\sigma_{\pi p}$  and  $\sigma_{\pi n}$  for  $\pi^-$ -meson interactions with protons and neutrons. A is the atomic weight, Z the atomic number and R the nuclear radius of the particular element. By the principle of charge independence, the cross-sections  $\sigma_{\pi n}$  and  $\sigma_{\pi p}$  are equal, and for meson energies below 300 MeV the ratio  $\sigma_{\pi p}$  to  $\sigma_{\pi n}$  is 3. (See fig. 1). Writing R as  $r_0 A^{1/3}$ , the expression for K becomes

$$K = 3/4\pi r_0^3 \cdot \sigma_{\pi p} (3 - 2Z/A) \quad (7)$$

The dependence of K on Z and A leads to slightly different values for each constituent element of nuclear emulsion.



This difference, for the extreme elements of carbon and silver, is about 10%.

In this calculation it is assumed that all energy transfers between the incident particle and the constituent nucleons are possible, but the limitation imposed by the Pauli exclusion principle leads to a reduction in the value of K. At 88 MeV, because the momentum of the incident mesons is of a similar magnitude to that of nucleons with the maximum Fermi energy ( $\sim 20$  MeV), there is no simple way of allowing for the effect. However, absorption of the meson will take place and this leads to an increase in K. Cronin et al (1957) have investigated these two effects for 970 MeV  $\pi^-$ -mesons and different types of nuclei, and found them to be approximately equal in magnitude. Since the two effects are of opposite sign they will tend always to cancel each other, and for the purposes of this calculation, the value of K will be taken as being given by equation (7).

If it is assumed that absorption by nucleon pairs alone occurs, the absorption co-efficient is given by

$$K = 3 N_D \sigma_D / 4 \pi R^3 \quad (8)$$

where  $N_D$  is the number of effective nucleon pairs and  $\sigma_D$  is the absorption cross-section of deuterium. From the analysis of Brueckner et al (1951) it appears that  $N_D$  is equal to  $\Gamma Z$  where  $\Gamma$  is of the order of 10. Thus

$$K = 3\Gamma\sigma_2 / 8\pi r_0^3 \quad (9)$$

To the extent that  $\Gamma$  is constant, the absorption co-efficient is the same for each element contained in nuclear emulsion.

The total cross-sections for inelastic interaction and elastic or diffraction scattering are

$$\sigma_a = \pi R^2 \left[ 1 - 1/2 K^2 R^2 \left\{ 1 - (1 + 2KR) e^{-2KR} \right\} \right] \quad (10)$$

$$\begin{aligned} \sigma_d = \pi R^2 \left[ 1 + 1/2 K^2 R^2 \left\{ 1 - (1 + 2KR) e^{-2KR} \right\} - \right. \\ \left. 1/(K^2/4 + k_i^2)^2 R^2 \left\{ (K^2/4 - k_i^2) + e^{-KR} \left[ 2k_i R (R^2/4 + k_i^2) + k_i K \right] \sin 2k_i R - \right. \right. \\ \left. \left. e^{-KR} \left[ (K^2/4 - k_i^2) + KR (K^2/4 + k_i^2) \right] \cos 2k_i R \right\} \right] \quad (11) \end{aligned}$$

as given by Fernbach. The differential cross-section is

$$d\sigma_d/d\Omega = \sigma_d/\pi \left[ J_1(KR \sin \theta) / \sin \theta \right]^2 \left[ (1 + \cos \theta) / 2 \right]^2 \quad (12)$$

where  $J_1$  is the first order Bessel function and  $\theta$  the spatial angle of scatter. This equation is an approximation in the limit  $KR \rightarrow \infty$ . In practice  $KR \approx 2$ , but calculations using this and a more exact expression yield angular distributions agreeing to better than 10%.

Equation (12) differs from that given by Fernbach in the incorporation of the obliquity factor  $\left[ (1 + \cos \theta) / 2 \right]^2$  (Brenner and Brown, Fowler and Perkins, private communication). It is, however, not important at high energies where the elastic scattering is confined to small angles.

At low energies the meson wavelength becomes comparable with the nuclear size and this requires a further correction. From Feshbach and Weisskopf (1949), the

maximum total cross-section corresponding to a 'black' nucleus is given by  $2\pi(R+\lambda)^2$  where  $\lambda$  is the reduced de Broglie wavelength of the meson. The cross-sections of equations (10) and (11) are then modified to

$$\left. \begin{aligned} \sigma_a' &= (\sigma_a^i + \pi^{\frac{1}{2}} \lambda)^2 \\ \sigma_d' &= (\sigma_d^i + \pi^{\frac{1}{2}} \lambda)^2 \end{aligned} \right\} \quad (13)$$

### 2.3. Application to Nuclear Emulsion.

Nuclear emulsion has eight constituent elements - hydrogen, carbon, nitrogen, oxygen, sulphur, bromine, silver, iodine-and the contributions to the diffraction scattering of each of these nuclei must be considered. If there are  $N_i$  nuclei per  $\text{cm}^3$  of the  $i$ th element each having a cross-section  $\sigma_i$ , then the mean cross-section,  $\bar{\sigma}$ , for elastic or inelastic processes is given by

$$\bar{\sigma} = \sum N_i \sigma_i / \sum N_i \quad (14)$$

It is the sum of the several cross-sections  $\sigma_i$  according to their frequency of occurrence. Experimentally, the quantity determined in emulsion is the interaction length  $\lambda$  given by

$$\lambda = 1 / \sum N_i \sigma_i \quad (15)$$

and the experimental value for inelastic interaction may be compared directly with the predictions of the optical model, leading to a value for  $K$ , the absorption coefficient.

A similar comparison of the cross-section for elastic scattering or the angular distribution determines  $k_1$ . This is made difficult by the practical inefficiency of detection of small angles, and by contamination from Rutherford scattering. Nevertheless, a value can be obtained by fitting theoretical angular distributions to the experimental distribution where these effects are unimportant. The observation of Rutherford scattering affords a means of determining the sign of the nuclear potential. If the angular distributions for  $\pi^+$ - and  $\pi^-$ -mesons are compared in the appropriate region, the effects of interference between the Coulomb and nuclear potentials can be observed. (Williams et al, 1956a,b,) In the one case an increase in the differential cross-section is observed where the potentials have the same sign; in the other the cross-section is correspondingly reduced.

### CHAPTER 3

#### SOME ASPECTS OF NUCLEAR EMULSION TECHNIQUE

Detailed accounts of the technique have been given by Voyvodic (1954), Shapiro (1958) and Bonet<sup>t</sup>/<sub>1</sub> et al, (1958); the discussion here is confined to those aspects which concern the present experiment.

##### 3.1 Processing of Emulsions

The processing of nuclear emulsions is an important feature of any experiment involving their use, since it is at this stage that the quality of the developed image is determined.

With emulsions of a thickness greater than 50  $\mu\text{m}$  a way must be found of ensuring a uniform development; if normal photographic methods are employed, a greater degree of development is obtained at the surface owing to the considerable penetration time of the solution through the emulsion. The most satisfactory means of overcoming this difficulty makes use of the more rapid temperature variations of development compared with penetration time. The emulsions absorb the solution at low temperatures, and development begins when the temperature is raised to a suitable level, depending on the degree of development required. A uniform cessation is obtained by reducing the temperature to the original low value. A variety of developing solutions

have been used including dilute photographic developers such as Ilford I. D. 19. It has been shown, however, Herz. (1952), that the best contrast between particle tracks and background grains, as well as the most rapid penetration time, is obtained with an amidol developer. The fixing of the plates is similarly more complicated than in photographic processing. The maximum rate of fixing is obtained with a 30% solution of hypo and the osmotic pressure resulting from a sudden transfer to pure water would cause the complete disruption of the emulsion. A slow dilution of the fixing solution is therefore employed, but even so it is not always possible to avoid the appearance of small bubbles.

In this experiment, a block of Ilford G5 emulsion made up of 20 strips, each 20 cm x 10 cm x 0.04 cm, was exposed to the 96 MeV  $\pi^-$ -meson beam of the Liverpool synchrotron. A particle flux was obtained on the end face of the block of about  $10^4$  mesons per  $\text{cm}^2$ . Throughout the period of transit and exposure the plates were maintained at constant humidity, having a relative value of 55% at 19°C. Before carrying out the processing of the complete block a series of trial developments were undertaken to determine the optimum conditions. A grain density for the incident mesons of about 22 grains per 100  $\mu\text{m}$  was considered appropriate, and as an additional consideration it was desirable to have as small a background as possible of single developed grains.

The most important of the parameters that can be varied in the processing cycle are the temperature and duration of the hot stage. An increase of  $1^{\circ}\text{C}$  in the former results is an increase of about 0.5 grains per  $100\text{ }\mu\text{m}$  in the grain density of tracks of plateau ionization. The chief effect of a greater duration of the hot stage above some minimum value is to produce an increased grain size, especially of the background grains. The effects of the two parameters, however, are linked to a considerable degree, and trial and error necessarily play a greater part in determining their values for any particular experiment.

A standard temperature cycle method of processing was employed. To begin with, each emulsion pellicle was mounted on glass, using for the purpose a special solution consisting of equal quantities of air-free distilled water and absolute ethyl alcohol, with 20 ml per litre of solution of glycerine and 1 ml per litre of a wetting agent. The solution, cooled to  $5^{\circ}\text{C}$ , was used to moisten the glass plates and the under surface of the emulsions; the latter were then attached to the plates by rolling with a rubber squeegee which carried a load of 2.5 Kg. to supply a constant pressure. The plates were stacked under a 1 Kg. weight and, when dry, were placed in a bath of distilled water at  $5^{\circ}\text{C}$ . A

time of  $1\frac{1}{2}$  hours was sufficient for the emulsions to become saturated and they were then removed to amidol developer at the same temperature for a further hour and a half. Having thoroughly absorbed the solution, the plates were taken out, excess liquid being removed by blotting, and placed on trays in a thermostatically controlled enclosure at  $24^{\circ}\text{C}$ . Eighty minutes later, development was curtailed with a stop bath of a solution of 0.5% glacial acetic acid at  $5^{\circ}\text{C}$ , and after a further period of  $1\frac{1}{2}$  hours the plates were removed to a solution of 30% hypo at the same temperature. This was replaced with fresh solution, also at  $5^{\circ}\text{C}$ , on two occasions at intervals of about 6 hours; on the second occasion 2% of sodium sulphate was added to the hypo for the purpose of hardening the emulsion. Fixing took in all some 22 hours to complete and was followed by a gradual dilution of the solution with water. As a result of the slow reduction of the hypo concentration at a rate of about 1% per hour, bubbling of the emulsion was negligible. The plates were thoroughly washed to remove all trace of hypo, then placed in a bath of 2% glycerine for 1 hour. This plasticizing of the emulsions was done to prevent later stripping from the glass backing. It is possible by increasing the amount of glycerine, (up to 10%), to restore the emulsion to its original thickness; with a 2% solution the shrinkage factor was about 2.3. Finally the plates



were removed from the bath and, after being carefully blotted, dried in the forced draught provided by an electric fan.

As a result of the development, the curvature distortion vector had the fairly high value of  $\sim 50 \mu\text{m}$ . Normally, before processing and while still intact, the block of stripped emulsions is exposed to a hard X-ray beam in such a way that, after development, small marks may be seen at selected points on the edges of the emulsion which correspond exactly throughout the block. By this means the matching of the separated plates after development is facilitated. This X-ray treatment, though carried out, was in this case unsuccessful, owing to a too low intensity of the X-ray beam. The plates were aligned, therefore, by tracing tracks from one to another, giving superposition to about  $500 \mu\text{m}$  only. The means of alignment are two reference edges of the glass backing the emulsion, which are cut so that location on the microscope stage against a point and a straight edge brings corresponding points of each plate into the same field of view.

### 3.2 Measurements in Emulsion

The identification of the particle responsible for a particular track in the emulsion depends on the measurements which can be made on that track. These are its

range, multiple scattering and ionization, which are related to the mass, charge and energy of the particle in question. Well-established formulae exist, determined by theoretical and empirical means, relating the former and latter quantities (Voyvodic, 1954). In general, a measurement of any two of the three quantities is sufficient for identification of the particle, but only within certain limits of the kinetic energy.

In this experiment it was planned to analyse the star data with regard to the identification of secondary  $\pi$ -mesons and a possible determination of a detailed energy balance. At 88 MeV secondary tracks may be expected to consist entirely of fairly low energy protons with a very small fraction of  $\alpha$ -particles, accompanied in certain cases by the emerging incident meson. It was possible in a large majority of cases to determine the complete range of the proton tracks and thus an exact value for their energy. In cases where the proton left the stack before reaching the end of its range, the shortness of path in the emulsion was usually a result of the steepness of the track, and therefore other measurements such as grain counting and scattering were not easily applicable. In such cases an estimate of the grain density at the beginning of the particle range was used to obtain a value of the momentum from a calibration curve which had been constructed using proton tracks of

known energy.

In most instances an immediate identification of secondary mesons could be made from the greater multiple scattering of the track compared with that of a proton. In about half the cases the meson could be followed to the end of its range, frequently in a  $\sigma$ -star, and the energy thus determined. Where this was not possible, grain density measurements were relied on as for protons, although in one or two instances, sufficient length of track was present in a single emulsion for a scattering measurement to be feasible. The value of the normalized grain density ( $g^*$ ) corresponding to the maximum possible energy of a secondary proton was about 1.8, and mesons of this grain density were easily distinguishable by inspection of the track. For lower values of  $g^*$ , the identification of meson could be safely assumed.

Measurements of particle range were carried out by recording the x,y, and z co-ordinates of the star of origin, the entry and exit points of each emulsion and the end point of the track. In addition, the co-ordinates were recorded of any point at which Coulomb scattering produced a change of direction. Correcting for shrinkage of the emulsion, the range was calculated with an error of about (2-3)%; the corresponding energy value was obtained from standard tables. (Fay et al, 1954) Where a grain counting

technique was employed, the error depended on the number of grains available, but was at best 10% and in a few cases as much as 40%. Measurements on multiple scattering gave momentum estimates to within (10 - 15)%.

## CHAPTER 4

### $\pi^-$ -MESON INTERACTIONS AT 88 MEV.

#### 4.1. Experimental Details

Four observers assisted in the scanning which was performed on Cooke M4000 microscopes under a magnification of  $45 \times 1.5 \times 15$ . By the method of track scanning employed, meson tracks selected at a distance from the emulsion edge of exactly 1 cm, were followed to an interaction, out of the plate or for a maximum length of 1 cm. The purpose of this limitation was to keep the energy loss small. Thus the energy of the beam at the beginning and end of the 1 cm strip was calculated to be 93 and 86 MeV with an average value of 88 MeV. The average length of a track followed varied between observers with a mean value of 0.6 cm, and a mean length of 60 cm scanned per man-day was achieved. The selection of tracks to be followed was limited to those lying within  $\pm 6^\circ$  of the general beam direction. An eye-piece hair-line, aligned on each track to be followed, was readjusted at frequent intervals in view of the considerable multiple scattering.

Denoting by  $n_s$  the number of shower particles ( $g^* < 1.5$ ) and by  $n_h$  the number of heavily ionizing particles ( $g^* > 1.5$ ), an initial classification of observed interactions was made into two groups; those of type ( $n_h = 0, n_s = 1$ ) classed as elastic scatters, and the remainder as stars. With this

classification, inelastic interactions of type ( $n_h=0, n_s=1$ ) are included as elastic scatters. If the number of such events is comparable with the number of stars of type ( $n_h=1, n_s=1$ ), then the total number of stars will be underestimated by about 5%.

Included in the star group were 22 of type ( $n_h=1, n_s=1$ ) and after closer scrutiny three of them were identified as elastic interactions with a visible recoiling nucleus. An examination of the dynamics of these three showed them to be  $\pi^-p$  collisions and they were classed therefore as elastic scatters. Also included in the group were events of type ( $n_h=0, n_s=0$ ), disappearances of the meson in flight. The emulsion region up to 150  $\mu$ m around each of these was carefully examined for secondary tracks/or a continuing primary.

Following a preliminary visual estimate of star size, each star was re-examined in a search for possible secondary  $\pi$ -mesons. A majority of secondary prongs were black and of limited range, and could be identified at once as due to low energy protons. Black or grey tracks of greater range were followed through as many plates as necessary to permit identification. Tracks having an ionization near the plateau value presented a greater problem but were assumed as being due to mesons for reasons already mentioned. For each star in which a meson secondary was identified as well as for 101 other stars selected at random, a complete

analysis was carried out. This involved the measurement of the spatial angle of each secondary track relative to the primary, and where appropriate its range or grain density.

Measurements on elastic scatters were carried out to an accuracy of  $1^\circ$  and only where the projected angle was greater than  $8^\circ$ . The latter limit was chosen to eliminate that part of the angular distribution formed chiefly by Rutherford scattering. It corresponds to a scattering parameter just equal to the average nuclear radius for G5 emulsion.

#### 4.2. Contamination.

At the time of exposure the synchrotron beam consisted of 82%  $\pi^-$ -mesons, 4%  $\mu$ -mesons and 14% electrons (Cassels, private communication), and it has been assumed that the track length followed was contaminated in these ratios. Some possible sources of spurious events resembling those produced by  $\pi^-$ -mesons are considered.

The contribution of the elastic scattering of electrons to the spatial angular distribution above  $8^\circ$  was calculated from the Mott formula for a point nucleus. For the beam momentum of 180 MeV/c the contamination is estimated to be about 1%.

The interaction of the  $\mu$ -meson is very weak and no spurious events were expected from this source. The

interaction cross-section of electrons with nuclei is known to be of the order of  $10^{-29} \text{ cm}^2$ , and thus should produce negligible contamination. However, the disappearance of two electrons tracks in a track length of 103 cm, has been observed by Barkas et al (1952) at this same momentum. Such events would simulate the  $\pi^-$ -meson disappearance, but as the statistical weight for this type of event is low, no correction has been made. It may be noted that this could lead to an overestimation by about 5% of the inelastic cross-section.

### 4.3 Experimental Results.

#### 4.31. The Interaction Lengths.

In a total track length of 92.51 m, there were found 235 elastic scatters with horizontally projected angles larger than or equal to  $8^\circ$ , and 371 stars, this figure including 92 disappearances. After correcting for the beam contamination of 18%, the interaction length for the production of inelastic events was  $(20.4 \pm 1.1) \text{ cm}$ , and for elastic scattering through a projected angle  $\phi \geq 8^\circ$ ,  $(32.3 \pm 2.1) \text{ cm}$ . The geometrical interaction length is 29.3 cm. The individual interaction lengths for the four observers were very similar for all types of event, indicating little relative inefficiency of detection.



#### 4.32. Comparison with Optical Model

In order to make a comparison with the optical model, the interaction length for inelastic events,  $\lambda_a$ , has been computed from equations (10), (13) and (15) as a function of the absorption co-efficient  $K$ . The nuclear radius was taken as  $r_0 A^{1/3}$  with  $r_0 = 1.35 \times 10^{-13}$  cm. From equations (7) and (8) the value of  $K$  is expected, at a particular energy, to be constant to within 10% for all emulsion nuclei with the exception of hydrogen, for which the value is about half that for the other elements. However, because of the small size of the hydrogen nuclei, their contribution to the interaction length is small; thus  $K$  is assumed constant.

In curve A of fig. 3 is shown the dependence of  $\lambda_a$  upon the absorption co-efficient. In curve C correction has been made for the meson wavelength. For purposes of comparison, curve B shows the increase in cross-section due to Coulomb attraction compared with the uncorrected cross-section of A. This correction, however, is only valid when the meson wavelength is small compared with the nuclear size and none has been made to curve C. Using curve C of fig. 3, the experimental value of the interaction length yields an estimate of the absorption co-efficient of  $K$  equal to  $(4.0 \pm 2.5) \times 10^{12}$  cm<sup>-1</sup>.

Using this value for the absorption co-efficient, the horizontally projected angular distribution for scattering

was computed for assumed values of the change in wave number  $K$ , equal to  $(0, \pm 1, \pm 2) 10^{12} \text{ cm}^{-1}$ , corresponding to various values of the real nuclear potential. The existence of Rutherford scattering at angles of about  $8^\circ$  has already been referred to, and a preliminary comparison of the experimental angular distribution with the calculated ones indicated that this would cause an increase in the differential cross-section. An approximate correction was made by adding the estimated angular distribution for Rutherford scattering for projected angles greater than or equal to  $8^\circ$ . The increase implied a nuclear potential having the same sign as the Coulomb potential.

In fig 4 are shown the calculated distributions together with the experimental points, but from this graph it is possible to deduce only an approximate value of  $k$ . It may be obtained more precisely from a numerical integration of the functions shown, to determine the interaction length for elastic scattering through projected angles greater than or equal to  $8^\circ$  as a function of  $k$ . The experimental value of the interaction length corresponds to  $k$ , equal to  $-(1.86 \pm 0.20) 10^{12} \text{ cm}^{-1}$ . The error quoted here derives from the expected statistical uncertainty of the interaction length assuming that the absorption co-efficient is known exactly. The uncertainty in the determination of  $K$  leads to a further error of approximately  $\pm 0.04 \times 10^{12} \text{ cm}^{-1}$ , and is considered negligible.

Using equation (7) and assuming an average value of  $Z/A$ , an estimate of the free nucleon cross-section can be obtained from the value of  $K$ . This is  $(20^{+12}_{-4})\text{mb}$  and is quite consistent with the direct measurement at 88 MeV of Anderson et al (1952) of  $(21 \pm 9)\text{mb}$  and the more recent value at 96 MeV of Edwards et al (1959) of  $(21.9 \pm 0.7)\text{mb}$ . The three collisions on hydrogen observed correspond to a cross-section of about 10mb.

Considering the absorption mechanism alone, from equation (9) the approximate value for the cross-section  $\sigma_{\text{abs}}$  is  $(9^{+6}_{-2})\text{mb}$ . By virtue of charge independence this may be compared directly with a value obtained at 88 MeV by Rogers and Lederman (1957) of  $(7.0 \pm 1.4)\text{mb}$ , and is again consistent. It was found that some 15% of primary mesons emerged from the inelastic interactions and this suggests that both mechanisms contribute to the interaction process.

The attenuation length in nuclear matter of the meson wave,  $\lambda_n = 1/K$ , was found to be  $(2.5 \pm 0.6)10^{-13}\text{cm}$ . This corresponds to an imaginary component of nuclear potential,  $V_i$ , of  $-(32^{+20}_{-6})\text{MeV}$ .

Sternheimer (1956) has calculated the value of  $k$ , for a range of meson energies. At  $\sim 88\text{MeV}$ ,  $k$ , was found to be  $2.4 \times 10^{12}\text{cm}^{-1}$  in reasonable agreement with the value of  $k$ , above. The corresponding value of the real potential  $V_r$  is  $-(28 \pm 3)\text{MeV}$ . Some values of the nuclear potential

observed in other experiments near 88 MeV are shown in table 1.

TABLE 1

Values of  $V_r$  and  $V_i$  from experiments at energies close to 88 MeV.

Energy MeV	Particle	Target element	$V_r$ MeV	$V_i$ MeV	Reference
48	$\pi^\pm$	C	$-(15 \pm 15)$	$-(22 \pm 7)^\dagger$	Shapiro, 1951
62	$\pi^-$	G5		$\sim -19$	Ferretti, 1956
80	$\pi^+$			$\sim -24$	
120	$\pi^\pm$			$\sim -24$	
70	$\pi^\pm$	C	$\sim -18$	$\sim -9$	Byfield et al, 1952
78	$\pi^\pm$	Cu	$\sim -(35-45)$	$\sim -20$	Williams et al, 1956 a, b.
80	$\pi^+$ $\pi^-$	Al	$\sim -20$ $\sim -(30-40)$	$\sim -(10-25)$ Any value	Pevsner et al, 1955
88	$\pi^-$	G5	$-(28 \pm 3)$	$-(32^{+20}_6)$	Present work

$^\dagger$  Calculated from data in the paper.

Frank et al (1956) have made calculations of the real nuclear potential from free nucleon cross-section data. For kinetic energies of 60, 80 and 100 MeV, values of  $V_r$  of 20, 29, and 35 MeV respectively are obtained. A good comparison is made with the experimental figure given LaBore.

The above analysis was based on a square well potential of radius  $r_0 A^{1/3}$ , where  $r_0$  was chosen to be  $1.35 \times 10^{-13}$  cm for consistency with previous work of this nature (Clarke and Major, 1957). A weighted mean value of recent determinations is  $r_0 = (1.29 \pm 0.01)10^{-13}$  cm, which would lead to even broader distributions than those computed. For closer agreement a radius greater than  $1.35 \times 10^{-13}$  cm would have to be considered.

#### 4.33 The Inelastic Interactions

The 371 inelastic events are shown in table 2, classified according to the numbers  $n_h$  and  $n_s$  of heavily ionizing and shower particles.

TABLE 2

Distribution of star sizes according to  $n_h$  and  $n_s$ .

$n_h \backslash n_s$	0	1	2	3	4	5	6
0	92	88	76	51	29	11	1
1		15	5	2	1		

A second classification is made in table 3 according to the number of secondary  $\pi$ -mesons in each star.

TABLE 3.

Distribution of star sizes according to  $n_h$  and  $n_\pi$

$n_\pi \backslash n_h$	0	1	2	3	4	5	6
0	92	76	62	50	27	9	1
1	12	29	6	4	3		

At this energy, as has already been pointed out, any lightly ionizing particle must be a meson.

The mean value of  $n_h$  for the two types of star - with and without meson secondaries - is shown in table 4 together with values obtained by Ferretti et al (1956) for  $\pi^\pm$ -mesons at 120 MeV.

TABLE 4

Values of the mean number of prongs,  $\bar{n}$ , for stars with and without meson secondaries at 120 MeV (Ferrarri et al, 1956) and 88 MeV (present work).

	$\pi^+$ -mesons at 120 MeV	$\pi^-$ -mesons at 120 MeV	$\pi^-$ -mesons at 88 MeV
Stars without $\pi$ secondary.	$3.22 \pm 0.16$	$2.20 \pm 0.15$	$1.61 \pm 0.07$
Stars with $\pi$ secondary.	$1.18 \pm 0.21$	$1.20 \pm 0.17$	$1.20 \pm 0.15$

It can be seen that, where the incident meson escapes from the nucleus, the mean star sizes are roughly equal in the three cases, but where absorption takes place the results are significantly different. Scattering is most likely to occur on a proton for a  $\pi^+$ -meson and on a neutron for  $\pi^-$ -meson; the low energy recoil nucleon, having a large cross-section for interaction, may be expected to share its energy with the other nucleons of the nucleus, thus a similar type of star should result in either case. Where absorption takes place, this is assumed to be preferentially on a proton-neutron pair, producing two neutrons in the case of  $\pi^-$  absorption and two protons for  $\pi^+$  absorption. The energy of the nucleons will be sufficiently great for one of them to have a high probability of escaping, and since only the proton will be visible, a difference of one prong in the star sizes can be expected. At 120 MeV, more kinetic energy is available for transfer to the absorbing nucleus, and this will result in a larger mean star size.

A comparison is made in table 5 of values of  $n_h$  for the stars in which no charged meson secondary is observed with some recent results for  $\sigma$ -stars, i.e., absorption of  $\pi$ -mesons at rest. The comparison is limited to stars with one or more prongs because of the likely inefficiency of detection of zero prong  $\sigma$ -stars by the area scanning technique.

TABLE 5

Distribution according to  $n_h$  of stars with one or more prongs in which meson absorption has occurred at rest, and absorption or charge exchange at 88 MeV. The numbers are expressed as percentages.

$n_h=1$	2	3	4	5	6	No. of stars examined	Reference.
40.0	27.3	20.2	10.1	2.4	0.06	1038	Demeur et al (1956)
40.4	27.6	20.3	11.1	1.7	0.0	788	Brown and Hughes (1957)
40.1	26.7	21.7	9.7	1.6	0.2	983	Azimov et al (1957)
33.8	27.6	22.2	12.0	4.0	0.4	317	Present work.

The distributions are very similar despite the additional kinetic energy available in the 88 MeV stars; there is, as would be expected, a slightly higher percentage of stars with  $n_h \geq 4$  at the expense of those with  $n_h = 1$ . Of stars with  $n_h = 0$ , Menon et al (1950) found 28% and Demeur 35%, compared with 29% in the present experiment. The similarity of the results suggests that the same absorption mechanism operates in both cases.

15% of the stars were found to have inelastically scattered mesons and this value may be compared with one of 25% interpolated from the published results for 50 and 134 MeV of Metropolis et al (1958). These authors state, however, that no account has been taken of a meson-nucleus



potential which in this energy region means that the cross-sections  $\sigma_{\pi p}$  and  $\sigma_{\pi n}$  may have been underestimated by two or three times, resulting in a similar underestimation of the probability of absorption.

In fig 5 is shown the energy distribution of the secondary  $\pi$ -mesons. The preponderance of those in the lowest interval is due to a large proportion of quite steep tracks for which only a rough estimate of the grain density, that it was near to plateau, could be obtained. These particles were assigned a nominal zero energy loss, but should properly be spread over the first two energy intervals. Nikolskii et al (1957) give the energy distribution of 162 MeV  $\pi^-$ -mesons scattered inelastically into the angular interval  $(90-180)^\circ$  from stars found by area scanning. This is regular with a peak where the energy loss is about 70%, and bears a general resemblance to the distribution of fig 5.

The secondary mesons have been divided into two equal groups according to their greater or lesser energy loss, and a comparison of the mean size of the star of origin for each group is shown in table 6.

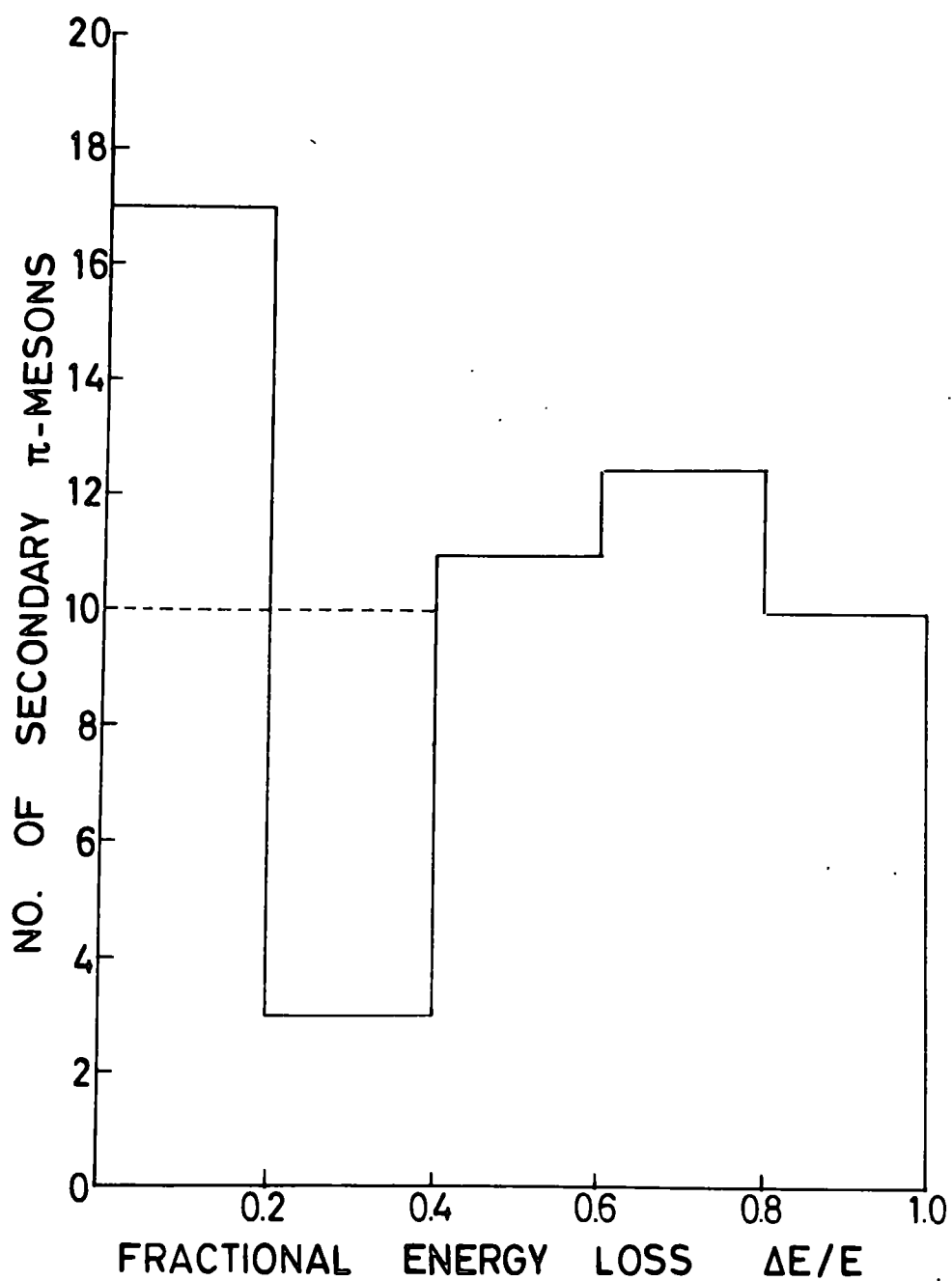


Fig.5. The energy distribution of the inelastically scattered mesons.

TABLE 6

Values of the mean energy loss ( $\overline{\Delta E}$ ) and fractional loss ( $\overline{\Delta E/E}$ ) of the secondary mesons and the mean number of prongs,  $\bar{n}_h$ , of the star of origin, with a division into two equal groups according to the greater or lesser energy loss of the meson.

	$0 < \Delta E/E < 0.58$	$0.58 < \Delta E/E < 1.0$
$(\overline{\Delta E/E})$ MeV	$0.16 \pm 0.04$	$0.75 \pm 0.17$
$(\overline{\Delta E})$ MeV	$14 \pm 3$	$66 \pm 15$
$\bar{n}_h$	$1.45 \pm 0.34$	$0.78 \pm 0.18$

A greater energy loss by the meson appears to result in a smaller star size. At 88 MeV the cross-section  $\sigma_{\pi n}$  is about three times as great as  $\sigma_{\pi p}$  and there will therefore be preferential production of neutron secondaries. In this energy region, the interaction cross-section for neutrons with nucleons decreases rapidly with increasing energy, and a neutron of higher energy, as might be produced in a more inelastic collision, will be able to escape more easily from the nucleus; thus the visible energy release in this case will be correspondingly less.

In fig 6 is shown the angular distribution of the secondary mesons. The distribution exhibits the expected peaks in the extreme forward and backward directions as

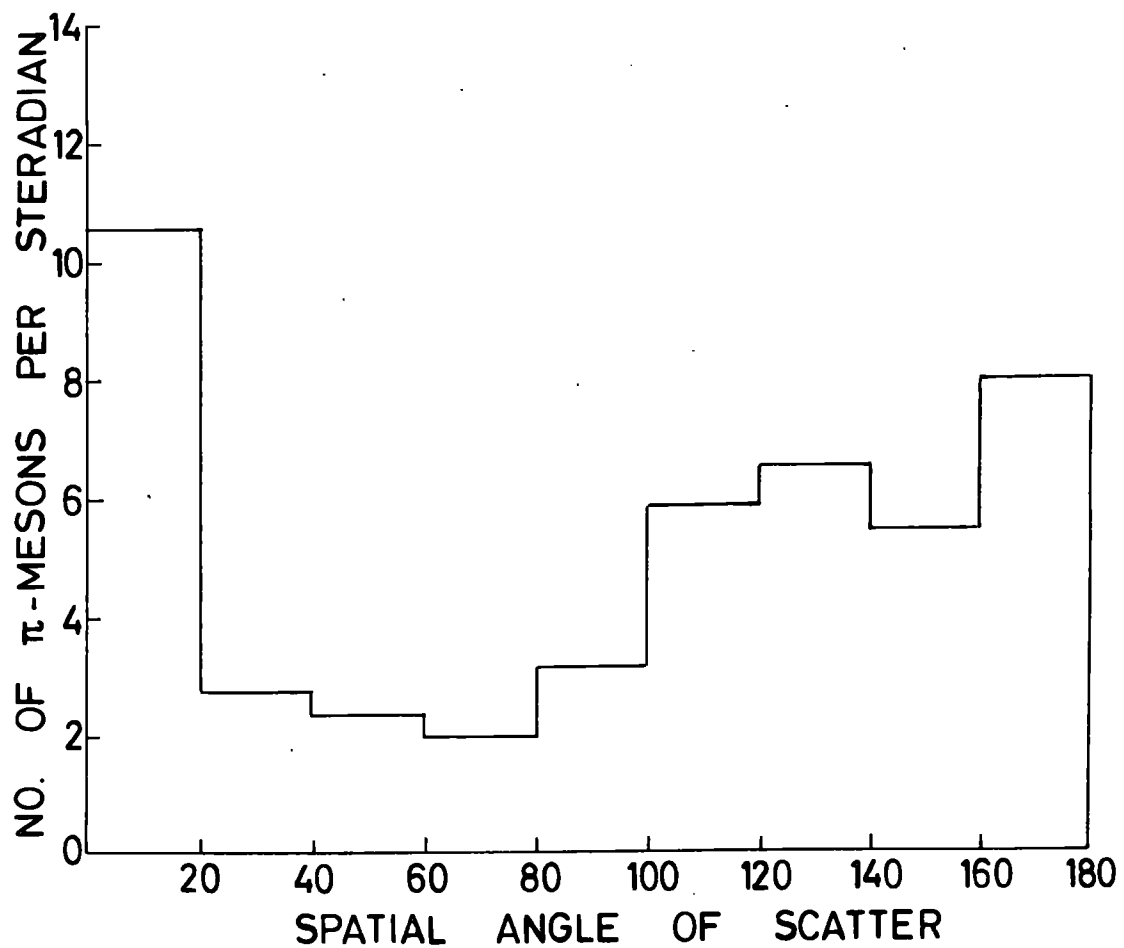


Fig.6. The angular distribution of the inelastically scattered mesons.

well as a broader maximum in the region of  $120^{\circ}$ . This latter is occasioned by the fact that the mesons producing steep tracks with small energy loss already referred to fall largely in the interval  $(90 - 140)^{\circ}$ . The result, if significant, might be explained on the basis of a meson which makes a single collision with small energy loss having a high probability of escape only where the collision takes place on the nuclear periphery. If mesons exhibiting a large energy loss are assumed to have undergone multiple collisions, then a more isotropic distribution is expected for them. Nikolskii found a distribution in which the number of mesons increased with increasing angle, there being roughly twice as many scattered into the interval  $(140 - 180)^{\circ}$  as into  $(0 - 40)^{\circ}$ . From the presented distribution, the ratio of mesons emitted in the forward hemisphere to those in the backward can be estimated as  $(0.69 \pm 0.08)$ . At 135 MeV, Goldhaber and Goldhaber (1953) obtained 0.53 for the forward to backward ratio and these values may be compared with one of  $(0.50 \pm 0.15)$  for the present experiment.

For the random selection of 101 stars without visible meson secondaries, it has been possible to calculate the forward to backward ratio for black ( $g^* > 6.5$ ) and grey ( $1.5 < g^* < 6.5$ ) tracks; these are given in table 7.

TABLE 7

Values of the forward to backward ratio  $F/B$  and the mean number of prongs for black, grey and all heavy prongs of the 101 selected stars.

	Black	Grey	All prongs
$F/B$	$1.01 \pm 0.18$	$0.9 \pm 0.5$	$1.05 \pm 0.17$
$\bar{n}$	$1.46 \pm 0.12$	$0.15 \pm 0.04$	$1.60 \pm 0.13$

It is seen that the angular distribution for both black and grey tracks is not significantly different from isotropic; this would be expected if the secondary particles were emitted as a result of absorption of the primary meson. The distribution may be compared with that for the stars containing an inelastically scattered meson. In these 54 events only two grey tracks were found, both emitted in the forward direction, and for black tracks the forward to backward ratio is  $(2.1 \pm 0.5)$ . The average star size  $(1.20 \pm 0.15)$  is, as would be expected, smaller than for absorption events. The nature of the differences in the characteristics of the two types of star suggests that charge exchange events form at most a very small proportion of those not identified as inelastic scattering events.

Because of the difficulty of estimating the considerable proportion of energy carried away by neutral secondary particles, no detailed energy balance has been carried out. Brown et al (1949) found that the empirical formula for the total energy release

$$E_s = 37n_h + 4n_h^2 \quad (16)$$

fitted closely their results from cosmic ray stars induced by energetic neutrons, as well as by charged particles, over a range of  $n_h$  from 4 to 24. Although apparently valid over a wide energy range for stars of mixed origin, it cannot be assumed to be so in the particular case of low energy negative  $\pi$ -mesons, because of the large probability for the production of secondary neutrons. As yet, therefore, it has been found not possible to estimate the contribution of charge exchange scattering to the absorption cross-section at this energy. If it is reasonably assumed insignificant, the percentage probabilities for inelastic scattering and absorption are respectively  $(15 \pm 2)\%$  and  $(85 \pm 5)\%$ . It has already been pointed out that the calculations of Metropolis may be in error with regard to the percentage of mesons absorbed; however, his estimate of the relative numbers emitted of charged and neutral mesons should be affected by this to only a very small extent. Using his value for the ratio of  $\pi^0$  to  $\pi^\pm$  of 0.45, the probability for charge exchange scattering so obtained is  $(6 \pm 2)\%$  and the

value for absorption becomes  $(79 \pm 5)\%$ . These figures have been incorporated in fig 2.



CHAPTER 5CONCLUSION

It has been shown that the optical model of Fernbach, incorporating the modifications of relativistic and obliquity factors, provides a satisfactory account of the interactions of  $\pi^-$ -mesons with complex nuclei at 88 MeV. The value of the change in wave number,  $k_1$ , was found to be  $-(1.86 \pm 0.20)10^{12} \text{ cm}^{-1}$  and the absorption co-efficient,  $K$ ,  $(4.0^{+2.5}_{-1.0})10^{12} \text{ cm}^{-1}$ . These gave values for the real and imaginary components of nuclear potential of  $V_r$  equal to  $-(28 \pm 3) \text{ MeV}$  and  $V_i$  equal to  $-(32^{+20}_{-6}) \text{ MeV}$ .

All evidence obtained from the inelastic interactions suggests the correctness of the cascade model in this energy region, and no serious disagreement has been found with an absorption mechanism involving proton-neutron pairs. It is concluded that of the inelastically interacting  $\pi$ -mesons, some 15% are scattered and the remaining 85%, except possibly for 6% emitted as neutral mesons, are absorbed into the nucleus.

The study of similar  $\pi$ -meson interactions at other, higher energies is expected to provide results of interest; some progress has already been made with an analysis of interactions at 750 MeV. From the results of the present work it seems that a comparison with  $\pi^+$ -meson interactions at the same energy values would help further towards understanding the exact nature of the inelastic collisions of  $\pi$ -mesons with atomic nuclei.

ACKNOWLEDGEMENTS

The author wishes to thank Professor G. D. Rochester for his unfailing encouragement and advice. He is indebted to Professor J. M. Cassels and his staff for permission to make an exposure on the Liverpool synchrotron and for much helpful assistance in carrying it out. He wishes further to express his indebtedness to his colleagues at Durham; in particular to Dr J. V. Major and Dr A. J. Apostolakis for many helpful discussions, and to Miss E. Perez-Ferreira and Mr Y. T. Lee for assistance with the scanning of the emulsion stack. The D.S.I.R. are thanked for a research award.

REFERENCES

- \* Allen J. E., Apostolakis A. J., Lee Y. J., Major J. V. and Perez-Ferreira E., 1959, Phil.Mag. 4, 858.
- Anderson H. L., Fermi E., Long A.E., Martin R., and Nagle D. E., 1952, Phys. Rev., 85, 934.
- Ashkin J., Blaser J. P., <sup>Feiner F.,</sup> Gorman J. C., and Stern M. D., 1954, Phys. Rev. 96, 1104.
- Azimov S. A., Guliamov U. G., Zamchalova E. A., Nizametdinova M., Podgoretskii M. I. and Iuldashev A., 1957, Soviet Physics (JETP) 4, 632.
- Barkas W. H., Deutsch R. W., Gilbert F. C., and Violet C. E., 1952, Phys. Rev. 86, 59
- \* Belovitskii G. E., 1958, Soviet Physics (JETP) 8, 581.
- \* Bernadini G. and Levy F., 1951, Phys. Rev. 84, 610.
- Bethe H. A. and de Hoffman F., 1955, Mesons and Fields, Vol II. (New York: Row, Peterson & Co.)
- \* Blau M. and Caulton M., 1954, Phys. Rev., 96, 150.
- \* Blau M. and Oliver A. R., 1956, Phys. Rev., 102, 489.
- Bonetti A., Dilworth C. and Scarsi L., 1958, The Nuclear Handbook (London: G. Newnes Ltd.,) Section 18,I.
- Brown G. and Hughes I. S., 1957, Phil Mag. 2, 777.
- Brown R. H., Camerini V., Fowler P. H., Heitler H., King D.T. and Powell C. F., 1949, Phil. Mag., 40, 862.
- Brueckner K. A., Serber A. and Watson K. M., 1951, Phys. Rev., 84, 258.

Burrowes H. C., Caldwell D. O., Frisch D. H., Hill D. A.,

Ritson D. M., Schluter R. A. and Wahlig M. A.,

1959, Phys. Rev., Lett., 2, 119.

\* Byfield H., Kessler J. and Lederman L. M., 1952, Phys. Rev.,

86, 17.

Clark A. C. and Ruddlesden S. N., 1951, Proc. Phys. Soc. A, 64, 1064

Clarke J. O. and Major J. V., 1957, Phil. Mag., 2, 37.

Cool R., Piccioni O. and Clark D., 1956, Phys. Rev., 103, 1082.

Cronin J. W., Cool R. and Abashian A., 1957, Phys. Rev. 107, 1121

Demeur M., Huleux A. and Vanderhaghe A., 1956, Nuovo Cimento,

4, 509.

\* Dzhelepov V. P., Ivanov V. G., Kozadaev M. S., Osipen<sup>k</sup>ov V. T.,

Petrov N. I. and Rosakov V. A., 1957, Soviet Physics

(JETP), 4, 864.

Edwards D. N., Frank S. G. F. and Holt J. R., 1959, Proc. Phys.

Soc., 73, 856.

Fay H., Gottstein K. and Hain K., 1954, Suppl. Nuovo Cimento,

11, 234.

Fernbach S., Serber R. and Taylor T. B., 1949, Phys. Rev. ,

75, 1352.

\* Ferrari G., Ferretti L., Gessaroli R., Manaresi E., Pedretti E.,

Puppi G., Quarenì A., Ranzi A., Stanghellini A. and

Stantic S., 1956, Suppl. Nuovo Cimento, 4, 914.

Ferretti L., Gessaroli R., Puppi G., Quarani G., Ranzi A.,  
Stantic S. and Tomasini A., 1956, CERN Symposium,  
Vol.II, 308.

Feshbach H. and Weisskopf V. F., 1949. Phys. Rev., 76, 1550.

\* Fowler C. E., Fowler W. B., Shutt R. P., Thorndike A. M. and  
Whittemore W. L., 1953, Phys. Rev., 92, 135.

Frank R. M., Gammel J. L. and Watson K. M., 1956, Phys. Rev.,  
101, 891.

\* Goldhaber A. and Goldhaber S., 1953, Phys. Rev., 91, 467.

Herz A. J., 1952, J. Sci. Inst., 29, 60.

Ignatenko A. E., 1956, CERN Symposium Vol.II, 313.

\* Kessler J. O. and Lederman L. M., 1954, Phys. Rev., 94, 689.

\* Kozadaev M. S., Sulaev R. M., Filipov A. I., and Shcherbakov I. A.  
Soviet Physics (JETP), 4, 580.

Le Couteur K. J., 1950, Proc. Phys. Soc. A, 63, 259.

Lindenbaum S. J., 1957, Ann. Rev. Nucl. Sci., 7, 317.

\* Lock W. O. and Yekutieli G., 1952, Phil. Mag., 43, 231.

\* Major J. V., 1959, Ph.D Thesis, University of Manchester.

Menon M. G. K., Muirhead H. and Rochat O., 1950, Phil. Mag. 41, 583

Metropolis N., Bivins R., Storm M., Miller S. M., Friedlander G.  
and Turkevich A., 1958, Phys. Rev., 110, 204.

\* Miller R. H., 1957, Nuovo Cimento, 6, 882.

\* Morrish A. M., 1953, Phys. Rev., 90, 674.

\* Nikolskii B. A., Kudrin L. P. and Ali-Zade S. A., 1957, Soviet  
Physics (JETP), 5, 93.

- Pevsner A., Rainwater S., Williams R. E. and Lindenbaum S. J.,  
1955, Phys.Rev., 100, 1419.
- Rogers K. C. and Lederman L., 1957, Phys. Rev., 105, 247.
- \* Saphir G., 1956, Phys. Rev., 104, 535.
- \* Schein M., Fainberg J., Haskin D. M. and Glasser R. G., 1953, Phys  
Rev., 91, 973.
- Serber R., 1947, Phys. Rev., 72, 1114.
- Shapiro A. M., 1951, Phys. Rev., 84, 1063.
- Shapiro M. M., 1958, Handbuch der Physik (Berlin:Springer-Verlag)  
Vol. XLV, 342.
- Sternheimer R. M., 1956, Phys. Rev., 101, 384.
- \* Tenney F. H. and Tinlot J., 1953, Phys Rev., 92, 974.
- Tomasini A., 1956, Nuovo Cimento, 3, 160.
- Voyvodic L., 1954, Progress in Cosmic Ray Physics II, 217.
- \* Wang Kan-Chang, Wang Tso-Tsiang, Ding Da-Tsao, Dubrovskii L. N.,  
Kladnitskaya E. N. and Solov'ev M. I., 1959,  
Soviet Physics (JETP), 8, 625.
- Williams R. E., Baker, W. F. and Rainwater J., 1956a, Phys.  
Rev., 104, 1695.
- Williams R. E., Rainwater J. and Pevsner A., 1956b, Phys. Rev.,  
101, 412.
- Williams R. W., 1956, CERN Symposium, Vol II, 324.
- Yuan L. C. L., 1956, CERN Symposium, Vol.II, 195.

\* From these references were taken the data for fig. 2.

